PHYSICAL REVIEW E **76**, 036403 (2007)

Generation of strong quasistatic magnetic fields in interactions of ultraintense and short laser pulses with overdense plasma targets

Hong-bo Cai,[1,*] Wei Yu,[2] Shao-ping Zhu,[1] and Cang-tao Zhou[1]
[1]*Institute of Applied Physics and Computational Mathematics, P. O. Box 8009, Beijing 100088, China*
[2]*Shanghai Institute of Optics and Fine Mechanics, Shanghai 201800, China*
(Received 11 March 2007; revised manuscript received 7 June 2007; published 13 September 2007)

An analytical fluid model is proposed for the generation of strong quasistatic magnetic fields during normal incidence of a short ultraintense Gaussian laser pulse with a finite spot size on an overdense plasma. The steepening of the electron density profile in the originally homogeneous overdense plasma and the formation of electron cavitation as the electrons are pushed inward by the laser are included self-consistently. It is shown that the appearance of the cavitation plays an important role in the generation of quasistatic magnetic fields: the strong plasma inhomogeneities caused by the formation of the electron cavitation lead to the generation of a strong axial quasistatic magnetic field B_z. In the overdense regime, the generated quasistatic magnetic field increases with increasing laser intensity, while it decreases with increasing plasma density. It is also found that, in a moderately overdense plasma, highly intense laser pulses can generate magnetic fields $\sim$100 MG and greater due to the transverse linear mode conversion process.

DOI: 10.1103/PhysRevE.76.036403 PACS number(s): 52.38.Fz, 52.35.Mw, 52.50.Jm

I. INTRODUCTION

Recently, with the arrival of laser systems capable of delivering light pulses of extremely high intensities ($I_L\lambda_0^2 \geq 10^{20}$ W cm^{-2} μm^2) in the subpicosecond regime and with high temporal contrast, the problem of the generation of quasistatic magnetic (QSM) fields by laser pulses in plasmas has become one of the most important issues in the physics of the interaction of ultraintense laser radiation with plasmas [1–15]. This problem has interest both fundamentally and for applications, such as particle acceleration and inertial confinement fusion [16,17], x-ray generation, and the radiation of pulsars [18].

Such spontaneous magnetic fields can be generated by several mechanisms, including nonparallel density and temperature gradients in the ablated plasma [1], the ponderomotive force associated with the laser radiation itself [2,3], and the current of fast electrons generated during the interaction [4]. However, there still does not exist a well-established and satisfactory theory, in particular, for the generation of the QSM fields in overdense plasmas. Indeed, numerical simulations carried out by Wilks *et al.* [2] for the interaction of an ultraintense laser pulse with an overdense plasma target predict extremely high QSM fields, about 250 MG. Recently, QSM fields that are of the order of a few hundred megagauss have also been observed in the overdense region of an irradiated solid target by relativistic laser irradiation [5,6]. However, these immense fields cannot be properly explained on the basis of existing theories. Sudan [3] suggested that the spatial gradients, and the nonstationary character of the ponderomotive force, may lie at the origin of the strong azimuthal QSM fields. Kim *et al.* [7] and Berezhiani *et al.* [8] also pointed out that in interactions of ultraintense laser pulses with underdense plasmas the sources of axial magnetic field generation are the electron density and laser intensity inhomogeneities. Here, we attempt to extend their ideas to the case of overdense plasmas, and develop a systematic treatment of the phenomenon of the generation of QSM fields by relativistically strong laser pulses propagating in an initially uniform overdense cold plasma.

In the present paper, a self-consistent analytical model describing this scenario is presented. Our model, which is fully relativistic, includes the inward push and steepening of the plasma electron density profile by the light pressure of the ultraintense laser. That is, the electron density profile is determined self-consistently by the charge-separation field created by the inward compression of the electrons with respect to the stationary ions (which do not have time to react on the ultrashort laser-driven electron time scale) and the laser ponderomotive field [19,20]. When a high-intensity Gaussian laser pulse with a finite spot size irradiates an initially uniform plasma, the zero-frequency ponderomotive force of the electromagnetic radiation ($\nabla\gamma_0$) pushes out the plasma electrons from the region of its localization, and creates electron cavitation. The cavitation is surrounded by high-density shoulders which are due to the compression and shock formation as the cavitation is created. Since both the electron density N_0 and the relativistic factor γ_0 have a strong space dependence around the cavitation, the inhomogeneity of $\gamma_0^{-1}N_0$ will always lead to a large induced azimuthal current in the skin layer. It is also shown that only a circularly polarized laser pulse can produce such induced azimuthal currents, and therefore strong axial QSM fields B_z. Furthermore, in a moderately overdense plasma with initial plasma density several times the critical density, we found that transverse linear mode conversion happened, resulting in a strong axial QSM field as high as $\sim$100 MG. It should be stressed that, without the formation of the electron cavitation, the normal incidence of laser pulses will not lead to linear mode conversion. The formation of the cavitation is the key step in the generation of QSM fields in overdense plasmas [2]. Such a description is not yet available in the literature, to the best of our knowledge.

*caihonb@yahoo.com.cn

The paper is organized as follows. In Sec. II, the basic equations describing this scenario are presented. In Sec. III, the formation of the electron cavitation and the spatial contour of the laser amplitude are discussed. In Sec. IV, the transverse linear mode conversion and the generation of azimuthal current are discussed in detail. In Sec. V, the generation of the QSM fields and their dependence on the laser intensity and plasma density are analyzed. In Sec. VI, a summary of the results is given.

II. BASIC EQUATIONS

We consider an ultraintense and ultrashort Gaussian laser pulse with a finite spot size irradiating a solid-density plasma normally from the z direction. On this time scale ($t<1$ ps), the plasma density is not affected by the usual hydrodynamic plasma expansion. We shall assume an initial homogeneous plasma density at $z>0$, where $z=0$ is the vacuum-plasma interface. The ion motion during the process of interest is negligible and will be ignored. Furthermore, the quiver velocity of the electron in the laser field is much higher than the electron thermal velocity, so that the plasma can be assumed to be cold. Combining $\mathbf{B}=\nabla\times\mathbf{A}$ and Ampère's law, we obtain

$$c^2\nabla^2\mathbf{A}-\partial_t^2\mathbf{A}=4\pi cen_e\mathbf{u}+c\,\nabla\,(\partial_t\phi)+4\pi cen_e\mathbf{v}, \quad (1)$$

$$\nabla^2\phi=4\pi e(n-Zn_i), \quad (2)$$

where $\mathbf{u}$ and $\mathbf{v}$ are the transverse and longitudinal components of the electron velocity, satisfying $\nabla\cdot\mathbf{u}=0$ and $\nabla\times\mathbf{v}=0$, $\mathbf{A}$ and ϕ are the vector and scalar potentials satisfying the Coulomb gauge $\nabla\cdot\mathbf{A}=0$, n_e (n_i) is the electron (ion) density, and Z is the ion charge number. Starting from the equation of motion for electrons, we obtain

$$\mathbf{P}_\perp=(e/c)\mathbf{A}, \quad (3)$$

$$\partial_t\mathbf{P}_l=e\,\nabla\,\phi-mc^2\,\nabla\,\gamma, \quad (4)$$

where $\mathbf{P}_\perp=m\gamma\mathbf{u}$, $\mathbf{P}_l=m\gamma\mathbf{v}$, and the relativistic factor $\gamma=(1-\mathbf{u}^2/c^2-\mathbf{v}^2/c^2)^{-1/2}$. Since usually $|\mathbf{u}|\gg|\mathbf{v}|$, it becomes $\gamma=(1-\mathbf{u}^2/c^2)^{-1/2}\approx(1+|\mathbf{a}|^2)^{1/2}$, where $\mathbf{a}=e\mathbf{A}/mc^2$ is the normalized vector potential and ω_0 the laser frequency. We consider that the vector potential has the form $\mathbf{a}(z,r,t)=\mathbf{a}_0(z,r,t)+\tilde{\mathbf{a}}_1(z,r,t)$, where $\mathbf{a}_0(z,r,t)$ denotes the quasistatic part of the vector potential, and $\tilde{\mathbf{a}}_1(z,r,t)$ denotes the normalized vector potential, given by

$$\tilde{\mathbf{a}}_1(z,r,t)=\frac{1}{2}\mathbf{a}_1(z,r,t)\exp(-r^2/r_L^2)\exp[-(t-t_p)^2/t_L^2]\exp(i\omega_0 t) + \text{c.c.}, \quad (5)$$

where $r=\sqrt{x^2+y^2}$ is the radius in cylindrical coordinates, r_L is the spot size, and t_L is the pulse duration. In particular, $\mathbf{a}_1(z,r,t)=a_1(z,r,t)(\mathbf{e}_x+i\alpha\mathbf{e}_y)$, and $\alpha=\pm1$ denotes the circularly polarized laser. In such a case, the normalized amplitude in vacuum can be described by $\mathbf{a}_1(z,r,t)=a_L(\mathbf{e}_x+i\alpha\mathbf{e}_y)[\exp(ik_0z)+\exp(-ik_0z+i\varphi)]$, where $k_0=\omega_0/c$ is the wave number in vacuum, and a_L is the amplitude of the incident laser. It should be stressed that $\varphi=\varphi_r+i\varphi_i$. The real part denotes the phase shift and the imaginary part determines the damping of the reflected wave. Fourier expand γ, ϕ, n_e, and v, e.g., $\gamma(z,r,t)=\gamma_0(z,r)+\tilde{\gamma}_1(z,r,t)+\cdots$, with $\tilde{\gamma}_1(z,r,t)=\frac{1}{2}\gamma_1 e^{i\omega_0 t}+\text{c.c.}$, where

$$\gamma_0=\frac{\omega_0}{2\pi}\int_0^{2\pi}(1+|\mathbf{a}|^2)^{1/2}dt\approx(1+|a_1|^2)^{1/2},$$

$$\gamma_1=\frac{\omega_0}{2\pi}\int_0^{2\pi}(1+|\mathbf{a}|^2)^{1/2}\cos\omega_0 t\,dt=0.$$

For the zero-frequency component (denoted by the subscript 0) of the electron motion, $\partial_t\mathbf{v}_0\approx0$; therefore, Eqs. (2) and (4) give [19,20]

$$\nabla\gamma_0=\nabla\psi_0, \quad (6)$$

$$N_0-N_i=\partial_\xi^2\gamma_0+\nabla_\perp^2\gamma_0, \quad (7)$$

where $N_0=n_{e0}/n_c$, $N_i=Zn_i/n_c$, $\psi_0=e\phi_0/mc^2$, and $\xi=(\omega_0/c)z$, and in the derivation of Eqs. (6) and (7) and the following equations we also introduce these dimensionless quantities: $\tau=\omega_0 t$, $\tau_L=\omega_0 t_L$, $\rho=(\omega_0/c)r$, and $\rho_L=(\omega_0/c)r_L$. Equation (6) describes how, in the region where the electron density $N_0\neq0$, the ponderomotive force $\nabla\gamma_0$ must be compensated by the force of the longitudinal field due to space-charge separation. Equation (7) tells us that under strong laser radiation the electron density profile is determined by the zero-frequency ponderomotive force. Although a similar model has already been discussed [20–22], we will emphasize that the analysis of this physical problem is also applicable to the interaction of a high-intensity Gaussian laser pulse with a finite spot size with overdense plasmas, which is a three-dimensional problem. Furthermore, we know that, when a high-intensity Gaussian laser pulse with a finite spot size irradiates an initially uniform plasma, the zero-frequency ponderomotive force of the electromagnetic radiation ($\nabla\gamma_0$) pushes out the plasma electrons from the region of its localization, and creates electron cavitation. The formation of the electron cavitation therefore will cause a lot of interesting physics, e.g., the generation of QSM fields, which will be discussed in the following.

It is important to emphasize that in such overdense plasmas (at least tens of the critical density), it is difficult for an electrostatic plasma wave to develop, and the electromagnetic component dominates the 1ω wave equation. Therefore, we can safely neglect the electrostatic component $\nabla\phi_1$ and $\mathbf{v}$ in the 1ω wave equation for laser radiation. Note that $\mathbf{a}_1(\xi,\rho,\tau)$ is a slowly varying function of ρ, in contrast to $\exp(-\rho^2/\rho_L^2)$. Hence, $\partial_\rho[\mathbf{a}_1\exp(-\rho^2/\rho_L^2)]\approx\mathbf{a}_1\partial_\rho[\exp(-\rho^2/\rho_L^2)]$. On the other hand, $\mathbf{a}_0(\xi,\rho,\tau)$ and $\mathbf{a}_{1s}(\xi,\rho,\tau)=\mathbf{a}_1(\xi,\rho,\tau)\exp(-\rho^2/\rho_L^2)\exp[-(\tau-\tau_p)^2/\tau_L^2]$ are also supposed to be slowly varying in time, i.e., $\partial_\tau^2(\mathbf{a}_{1s}e^{i\tau})\approx(2i\partial_\tau\mathbf{a}_{1s}-\mathbf{a}_{1s})e^{i\tau}$. Under these approximations, the 1ω wave equation becomes

$$\partial_\xi^2 \mathbf{a}_1(\xi,\rho,\tau) + i\alpha_2 \mathbf{a}_1(\xi,\rho,\tau) + [1 - 4(1-\rho^2/\rho_L^2)/\rho_L^2 - N_0/\gamma_0]\mathbf{a}_1(\xi,\rho,\tau) = 0, \quad (8)$$

where $\alpha_2 = 4[(\tau-\tau_p)/\tau_L^2]$. From Eqs. (7) and (8), we can determine the whole spatial profile of the normalized vector potential. It should be mentioned that, since the zero-frequency electron density N_0 is a function of ρ under high ponderomotive pressure, Eq. (8) will have different solutions at different transverse positions ρ. Furthermore, the complex amplitude can be defined by $a_1(\xi,\rho,\tau) = a_r + ia_i$, where a_r and a_i denote the real and imaginary parts of the laser amplitude, respectively. Therefore, Eq. (8) can be rewritten into two coupled real equations: $\partial_\xi^2 a_r = \alpha_2 a_i + [N_0/\gamma_0 + 4(1-\rho^2/\rho_L^2)/\rho_L^2 - 1]a_r$, and $\partial_\xi^2 a_i = -\alpha_2 a_r + [N_0/\gamma_0 + 4(1-\rho^2/\rho_L^2)/\rho_L^2 - 1]a_i$, which are the wave equations for laser radiation. Together with Eqs. (6)–(8), we obtain

$$\partial_\xi^2 \gamma_0 = \gamma_0^{-1}\alpha_1[a_r\partial_\xi^2 a_r + a_i\partial_\xi^2 a_i + (\partial_\xi a_r)^2 + (\partial_\xi a_i)^2 - \alpha_1\gamma_0^{-2}(a_r\partial_\xi a_r + a_i\partial_\xi a_i)^2], \quad (9)$$

$$\nabla_\perp^2 \gamma_0 = -8\alpha_1(a_r^2 + a_i^2)(1 - 2\rho^2/\gamma_0^2\rho_L^2)/\gamma_0\rho_L^2, \quad (10)$$

where we have made use of the relations $\gamma_0 = \sqrt{1+\alpha_1|a_1(\xi,\rho,\tau)|^2}$ and $\alpha_1 = \exp(-2\rho^2/\rho_L^2)\exp[-2(\tau-\tau_p)^2/\tau_L^2]$. In Eqs. (6)–(10), we have also neglected the influence of the generated magnetic field. The reason is that the corresponding gyrofrequency is much smaller than the carrier frequency.

From the above analysis, we conclude that a possible stationary solution of the model equations considered may include a depletion region at the vacuum-plasma boundary, where ion charges are uncompensated. In this region, the ponderomotive force is unbalanced and pushes all electrons forward inside the plasma, thus shifting the actual electron plasma boundary from $\xi=0$ to a new position $\xi_b = f(\rho)$ (vacuum-plasma interface). The new interface $f(\rho)$ can be determined along with the constraint given by total charge conservation. The integral over the whole plasma space of Eq. (7) gives

$$\int_0^{f(\rho)} N_i d\xi = \int_{f(\rho)}^{\infty} (N_0 - N_i) d\xi = -(\partial_\xi \gamma_0)_{f(\rho)} + \int_{f(\rho)}^{\infty} \nabla_\perp^2 \gamma_0 d\xi, \quad (11)$$

which determines the position of the effective vacuum-plasma interface $\xi_b = f(\rho)$. If this constraint is not satisfied, the spatial profile of the electron density will not satisfy the quasineutrality condition. In the region $\xi < f(\rho)$, including the pure ion layer $[0 < \xi < f(\rho)]$, the electromagnetic field $a_1(\xi,\rho,\tau)$ corresponds to a vacuum solution. We note that, at the effective vacuum-plasma interface $\xi_b = f(\rho)$, the transverse electromagnetic fields are continuous, that is, the solutions of Eq. (8) must be matched to the vacuum solution [21,22] $a_1(f(\rho)^-,\rho,\tau) = a_1(f(\rho)^+,\rho,\tau)$, $\partial_\xi a_1(f(\rho)^-,\rho,\tau) = \partial_\xi a_1(f(\rho)^+,\rho,\tau)$; and at $\xi=\infty$ the boundary condition is that the wave is evanescent. Equations (8)–(11) can be solved numerically, and the self-consistent spatial variations of the vector potentials and the electron density can be obtained from these nonlinear equations.

III. FORMATION OF ELECTRON CAVITATION

In the highly relativistic regime $(a_L \gg 1)$, any spatial variation of the laser intensity will act to push electrons to the regions of lower intensity through the zero-frequency ponderomotive force, which can approach the thermal pressure $(N_e kT_e)$ at solid density $(10^{24}\ \mathrm{cm}^{-3})$. When a high-intensity Gaussian laser pulse with a finite spot size irradiates an initially uniform plasma, the zero-frequency ponderomotive force of the electromagnetic radiation $(\nabla\gamma_0)$ pushes out the plasma electrons from the region of its localization, and creates electron cavitation. In the axisymmetric case, we can express the effective interface of the electron cavitation as $\xi_b = f(\rho)$ (this has been discussed above). Note that, at different transverse positions ρ, the interface has different values. In the center of the spot $(\rho=0)$, the electrons are most strongly pushed since the laser intensity peaks here, i.e., $\max\{f(\rho)\} = f(0)$. Under such a strong laser pressure, the electrons in the cavitation are pushed a small distance into the target and piled up in a narrow region with $\xi > f(\rho)$, leaving behind a thin layer of ions in the electron cavitation $[N_0=0$ in the region $\xi < f(\rho)]$. For $\xi \geq f(\rho)$, the spatial profile of the electron density N_0 can be obtained from Eqs. (7), (9), and (10),

$$N_0 = \gamma_0^2(N_i + \nabla_\perp^2\gamma_0) + \alpha_1\gamma_0\{[4(1-\rho^2/\rho_L^2)/\rho_L^2 - 1](a_r^2 + a_i^2) + (\partial_\xi a_r)^2 + (\partial_\xi a_i)^2 - \alpha_1\gamma_0^{-2}(a_r\partial_\xi a_r + a_i\partial_\xi a_i)^2\}. \quad (12)$$

Equation (13) describes how the electrons are piled up by the zero-frequency ponderomotive force. Since the vector potential and its space derivative decrease rapidly in the overdense plasma, the electrons are only piled in the skin layer. Furthermore, it should be pointed out that, within the framework of the current model equations [which are being widely exploited for the problem of relativistic self-focusing of electromagnetic (EM) beams], one cannot prevent the occurrence of unphysical, negative values for the electron density when $|\nabla^2\gamma_0| \gg N_i$. This failure of the hydrodynamic model of a plasma is generally corrected by putting $N_e=0$ in the entire spatial region where $N_e < 0$ [8].

The ponderomotive force of a laser pulse with a small spot size will tend to expel electrons from the region of the axis, so-called “electron cavitation,” as shown in Fig. 1. However, it should be pointed out that the electron density never becomes strictly zero in the cavitating region, which is a limitation of the hydrodynamical model [8]. Fortunately, the electron density in this region turns out to be a few orders of magnitude smaller than its original value because of the relativistic laser intensity, and therefore the pure ion layer approximation in electron cavitation is applicable. The spatial variations of the vector potential can also be calculated numerically from Eqs. (8)–(11). As expected, in the region $\xi < f(\rho)$, the vector potential is a vacuum solution, while in the region $\xi > f(\rho)$ the vector potential decreases rapidly into the overdense plasma [23]; as shown in Fig. 2.

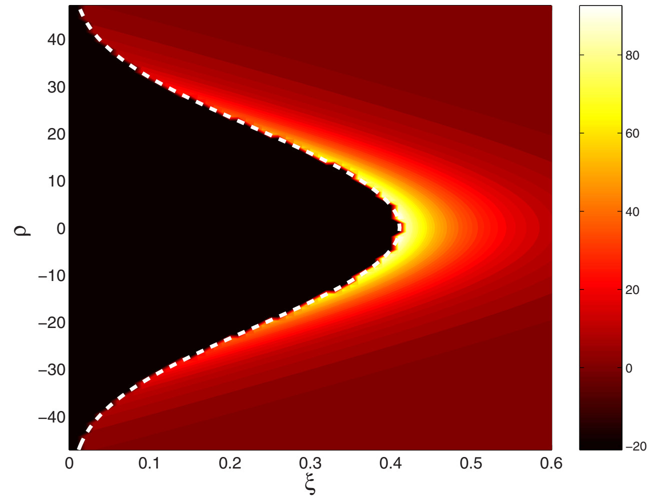

FIG. 1. (Color online) Spatial contours of the electric density (N_0-N_i) at $\tau=\tau_p$. Parameters are $a_L=5$, $\rho_L=5\lambda_0$, $\tau_L=30T_0$, $N_i=20$, and T_0 is the laser period.

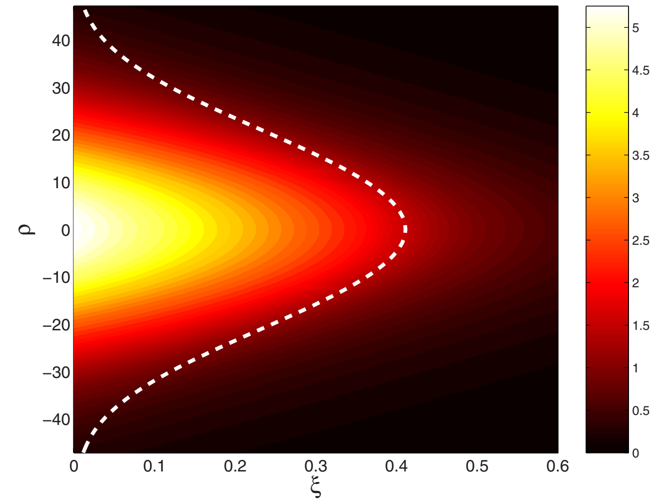

FIG. 2. (Color online) Spatial contours of the laser amplitude $|a_1(\xi,\rho,\tau)|\exp(-\rho^2/\rho_L^2)$ at time $\tau=\tau_p$. Here the white dashed line is the effective vacuum-plasma interface. Parameters are $a_L=5$, $\rho_L=5\lambda_0$, $\tau_L=30T_0$, $N_i=20$.

IV. GENERATION OF INDUCED AZIMUTHAL CURRENT

As with most problems involving fluids, one can write down a continuity equation for the mass, or in this case charge density: $\partial_\tau N_e+\nabla\cdot(N_e\mathbf{P}/\gamma_0)=0$. As in Sec. II, we Fourier expand N_e and $\mathbf{P}$ into $N_e=N_0+\widetilde{N}_1+\cdots$ and $\mathbf{P}=\mathbf{P}_0+\widetilde{\mathbf{P}}_1+\cdots$, with $\widetilde{N}_1(\xi,\rho,\tau)=\frac{1}{2}N_1e^{i\tau}+\text{c.c.}$ and $\widetilde{\mathbf{P}}_1(\xi,\rho,\tau)=\frac{1}{2}\mathbf{P}_1e^{i\tau}+\text{c.c.}$ Therefore, we obtain

$$\partial_\tau\widetilde{N}_1+\nabla\cdot(N_0\widetilde{\mathbf{P}}_1/\gamma_0)=0. \tag{13}$$

To obtain an equation for the 1ω electron density, we substitute $\partial_\tau\widetilde{\mathbf{P}}_1\cong-\widetilde{\mathbf{E}}_1=\partial_\tau\widetilde{\mathbf{a}}_1+\nabla\widetilde{\psi}_1$ and $\nabla^2\widetilde{\psi}_1=\widetilde{N}_1$ into Eq. (13) and then make use of the Coulomb gauge $\nabla\cdot\mathbf{a}_1=0$, to get

$$N_1=\nabla^2\psi_1=\frac{i\mathbf{a}_1\cdot\nabla(\varepsilon)}{\varepsilon}, \tag{14}$$

where $\varepsilon=1-N_0/\gamma_0$ is the dielectric function of the plasma. Note that as long as the laser electric field has a component along the gradient of ε linear mode conversion (LMC) occurs [24], which results in an electrostatic Langmuir oscillation N_1 at the laser frequency. Furthermore, Eq. (14) shows that the electron oscillation and hence N_1 are greatly enhanced as $N_0\sim\gamma_0$. Since in an overdense plasma the vector potential drops rapidly with distance into the plasma, the relativistic factor cannot be very large in the skin layer (as shown in Fig. 2). Therefore, from Eq. (14) we know that, if the initial plasma density is about several times the critical density, $N_i\in(1,5)$, the electron oscillation will be greatly enhanced. In the nonrelativistic regime, LMC is well studied for the oblique incidence of a p-polarized laser onto an inhomogeneous plasma layer [24,25]. As is known, the LMC is only for p polarization where the electric field has a component parallel to the $\mathbf{e}_\xi$ direction, the direction in which the density gradient is considered.

However, we found that LMC would happen even for a normally incident relativistic laser with a finite spot. Let us recall Sec. III and notice that electron cavitation is formed when such a relativistic laser pulse irradiates a plasma. Therefore, the electron density, both in the $\mathbf{e}_\xi$ direction and in the transverse directions to the laser propagation, may have spatial density gradients. Notice that the laser field oscillates in the transverse directions, therefore, LMC can occur for this case, and thus a 1ω electron density fluctuation is stimulated. However, it should be stressed that, without electron cavitation, the normal incidence of laser pulses will not lead to LMC. On the other hand, since the electrons are oscillating helically in the light wave with the velocity $\widetilde{\mathbf{u}}_1=\widetilde{\mathbf{a}}_1/\gamma_0$, an azimuthal current $J_\theta=\langle N_1\mathbf{u}_1\rangle_\tau$ is generated, where $\langle\cdots\rangle_\tau$ denotes averaging over the fast optical time scale. This is the physical explanation of the quasistatic azimuthal current.

Equation (14) can further give $N_1=-i\varepsilon^{-1}a_\rho\partial_\rho(\gamma_0^{-1}N_0)$. Here we have used the relation $\partial_\theta\to 0$, which means that the plasma-field structures are axisymmetric. Notice that the normalized vector potential also takes the form

$$\widetilde{a}_1(\xi,\rho,\tau)=(1/2)(\mathbf{e}_\rho+i\alpha\mathbf{e}_\theta)a_1(\xi,\rho,\tau)\exp(-\rho^2/\rho_L^2)\times\exp[-(\tau-\tau_p)^2/\tau_L^2]\exp(i\tau)+\text{c.c.},$$

where $\alpha=\pm1$ denotes a circularly polarized laser and $\alpha=0$ denotes a linearly polarized laser. Thus, the induced azimuthal current J_θ is given by

$$J_\theta=\frac{\alpha\langle\gamma_0^{-1}|a_1|^2\partial_\rho(\gamma_0^{-1}N_0)\rangle_\tau}{1-N_0/\gamma_0}. \tag{15}$$

As discussed above, from Eq. (15), we know that in a moderate-density plasma $[N_i\in(1,5)]$, the electrons are driven away from the center of the spot by the ponderomotive force of a laser pulse with a finite spot size, and piled in the skin layer. In this case, large induced azimuthal currents can be generated since the dielectric function $\varepsilon=1-N_0/\gamma_0$ is very small. Therefore, the maximum value of the axial QSM field turns out to be several hundreds of megagauss or even 10^9 MG [5]. It is important to stress that, in the limit $N_i\ll1$,

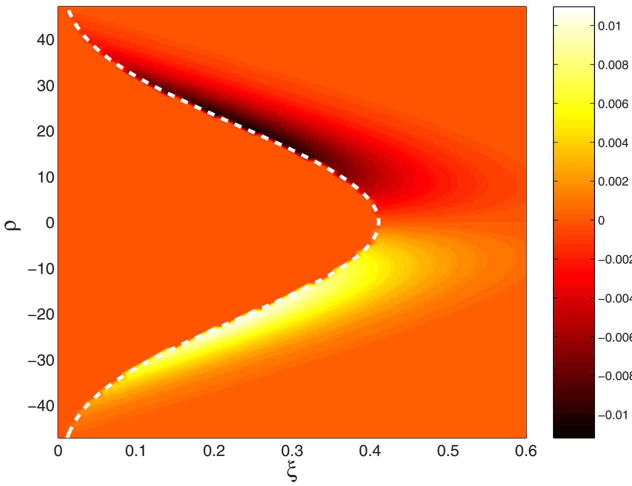

FIG. 3. (Color online) Spatial contours of the induced azimuthal current J_θ at time $\tau=\tau_p$. Here the white dashed line is the effective vacuum-plasma interface. Parameters are $a_L=5$, $\rho_L=5\lambda_0$, $\tau_L=30T_0$, $N_i=20$.

Eq. (15) can be approximated by $J_\theta=\alpha\langle\gamma_0^{-1}|a_1|^2\partial_\rho(\gamma_0^{-1}N_0)\rangle_\tau$, which recovers the relation discussed by Kim *et al.* [7] and Berezhiani *et al.* [8]. But an important difference is that, in our theory, the electric field may resonantly excite a large electrostatic plasma wave in the transverse directions, which results in large azimuthal currents and therefore strong axial QSM fields.

However, in the overdense regime ($N_i \gg 1$), much smaller induced azimuthal currents are expected since the dielectric function $\varepsilon=1-N_0/\gamma_0\approx -N_i$. It should be mentioned that, in our model, the density profile immediately adjacent to the cavitation may look like a jump, which means that large azimuthal surface currents might be generated on the boundary of the cavitation. However, in the case of a tightly focused relativistic laser pulse irradiating an overdense plasma, this resonance region is very narrow [6]. Therefore, only two oppositely directed azimuthal currents might be generated close to the resonance point $\varepsilon=0$ on this boundary. But one can easily see that the effects of such currents on the axial QSM field offset each other, so the collective effect of the currents on the boundary of the cavitation can be safely disregarded, and only the induced currents in the skin layer are dominant.

Figure 3 shows the spatial contours of the induced azimuthal current J_θ at time $\tau=\tau_p$ in an overdense plasma with $N_i=20$. Clearly, the induced quasistatic azimuthal current only exists in the skin layer around the cavitation. Furthermore, there is no azimuthal current at $\rho=0$ because $\partial_\rho(\gamma_0^{-1}N_0)$ is zero here. Such azimuthal currents will result in the generation of a strong axial QSM field, which peaks on the axis $\rho=0$. The physical explanation is the following. When a laser beam with a finite spot size propagates in an initially uniform plasma, the ponderomotive force of the EM radiation $(\nabla\gamma_0)$ pushes out the plasma electrons from the region of its localization, and creates an effective plasma density inhomogeneity. Since both the electron density N_0 and the relativistic factor γ_0 have a strong space dependence, the inhomogeneity of $\gamma_0^{-1}N_0$ will always lead to large induced azimuthal currents. Notice that only the circularly polarized laser pulse can produce the induced azimuthal currents, and therefore the axial QSM field B_ξ.

V. GENERATION OF QUASISTATIC MAGNETIC FIELDS

In the present work we deal with the generation of quasistatic magnetic fields by relativistically strong laser pluses irradiating overdense plasmas. In this case, we confine our attention to circularly polarized laser pulses for which axial QSM fields should appear according to the Ampère law. In the following we will show that the generation of the axial QSM fields takes place due to the formation of electron cavitation caused by the intense laser beam itself.

From Ampère's law $\nabla\times\mathbf{B}_0=\mathbf{J}_0+\partial_\tau\mathbf{E}_0$ and $\mathbf{E}_0=-\partial_\tau\mathbf{a}_0-\nabla\psi_0$, we have $\nabla\times\mathbf{B}_0\approx-\partial_\tau(\nabla\psi_0)+\mathbf{J}_0$. The quasistatic current $\mathbf{J}_0=\langle N_1\mathbf{u}_1\rangle_\tau$. Therefore, we obtain $\nabla\times\mathbf{B}_0\approx-\partial_\tau(\nabla\psi_0)+\langle N_1\mathbf{u}_1\rangle_\tau$. Substituting Eq. (14) into this equation, we obtain

$$\nabla\times\mathbf{B}_0\approx-\partial_\tau(\nabla\psi_0)-i\varepsilon^{-1}\langle\gamma_0^{-1}a_\rho\mathbf{a}_1\partial_\rho(\gamma_0^{-1}N_0)\rangle_\tau. \quad (16)$$

It is easy to interpret this equation physically. The first term on the right-hand side (RHS) of Eq. (16) is the usual displacement current term, which results in the generation of azimuthal QSM fields B_θ and has been analyzed in Ref. [3]. Here, we will focus on the generation of the axial QSM fields B_ξ in an overdense plasma. The second term on the RHS of Eq. (16) is the induced azimuthal current J_θ, which has a form analogous to the one considered in Refs. [7,8], where an underdense plasma was considered. In these papers [7,8], the plasma densities are assumed to be very low and thus the physical quantities can be assumed to be homogeneous in the propagation direction. However, our interest in this work is in the overdense regime, in which the longitudinal (propagation direction) variations of the vector potentials and electron density have to be considered. Furthermore, the denominator $\varepsilon=1-N_0/\gamma_0$ in Eq. (16) is missing in Refs. [7,8], and therefore the linear conversion process is not taken into consideration in that work.

Substituting Eqs. (6) and (7) into Eq. (16), the spatial variations of the axial QSM field B_ξ can be determined [8,11]. From the spatial distribution of the azimuthal current (see Fig. 3), we can expect that the strength of the magnetic field has a maximum value on the beam axis $\rho=0$ in the beam propagation area, then decreases, changes polarity, and rapidly tends to zero as $\rho\to\infty$. Here, what we care about mostly is the peak axial QSM field $B_{\xi m}\equiv\max\{B_\xi\}$.

Figure 4 shows how the peak axial QSM field $B_{\xi m}$ depends upon the incident laser amplitude for fixed initial plasma density N_i. One can see that at relativistic intensities $B_{\xi m}$ increases for fixed $N_i=20$ and growing intensity. Since higher intensity leads to stronger spatial inhomogeneity of the electron density, one can expect that $B_{\xi m}$ will be higher. However, it turns out that the higher electron density in the skin layer caused by the laser pressure eliminates this effect. As shown in Fig. 4, when $a_L>4$, the increase of $B_{\xi m}$ slows down. Figure 5 shows that the peak axial QSM field $B_{\xi m}$ decreases with increasing initial plasma density for fixed laser amplitude. One can see that on the whole $B_{\xi m}$ is only several megagauss, which cannot be as high as the magnetic

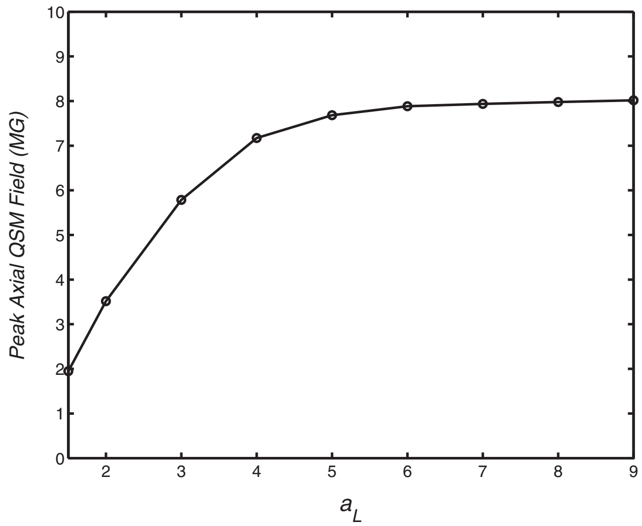

FIG. 4. Peak axial QSM field as a function of the incident laser amplitude. Parameters are $\rho_L=5\lambda_0$, $\tau=\tau_p$, $\tau_L=30T_0$, $N_i=20$.

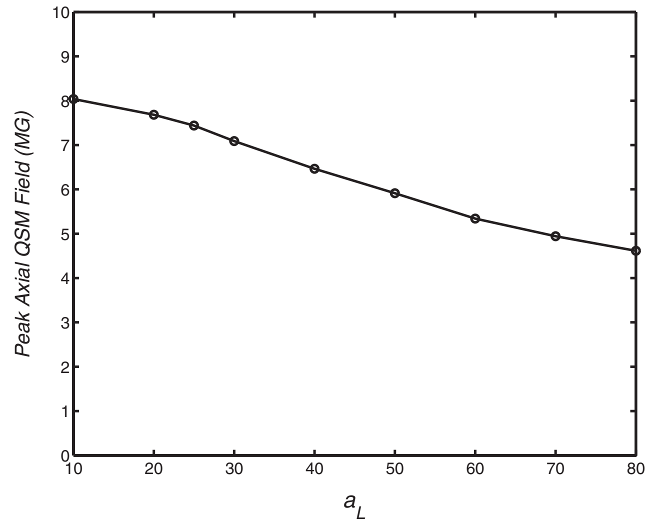

FIG. 5. Peak axial QSM field as a function of the initial plasma density. Parameters are $\rho_L=5\lambda_0$, $\tau=\tau_p$, $\tau_L=30T_0$, $a_L=5$.

field of laser radiation. However, in a moderately overdense plasma $[N_i\in(1,5)]$, the fields can be quite strong for high-intensity laser radiation since the transverse linear mode conversion process will happen.

VI. CONCLUSION

In conclusion, we have developed a self-consistent model to explore the generation mechanisms of the QSM field in interactions of ultraintense and short laser pulses with overdense plasmas. The model, spanning a large range of interaction conditions $(10^{18}\leq I_L\lambda_0^2\leq 10^{20}\text{ W cm}^{-2}\,\mu\text{m}^2,\ 10\leq N_i\leq 80)$, revealed that the formation of the electron cavitation plays an important role in the generation of the axial QSM field. Because of the strong plasma inhomogeneity caused by the formation of this cavitation, a low-frequency drag current is induced, $J_\theta=\alpha\varepsilon^{-1}\langle\gamma_0^{-1}|a_1|^2\partial_\rho(\gamma_0^{-1}N_0)\rangle$, which produces a large QSM field B_ξ in the beam propagation area, according to Ampère's law. In all of these cases, the axial QSM field peaks on the beam axis. Furthermore, we found that the laser intensity and the initial plasma density are crucial parameters: our results show that the QSM field increases with increasing laser intensity but decreases with increasing plasma density. It is also found that in an overdense plasma with $N_i\gg 1$, the QSM field is smaller than what was found in previous publications. In a moderately overdense plasma with $N_i\in(1,5)$, however, the generated QSM fields can reach considerable magnitudes since transverse linear mode conversion will happen.

However, it should be pointed out that, when the initial plasma density $N_i\in(1,5)$, the QSM fields can be as high as 10^8 G or greater; therefore, the corresponding gyrofrequency is of the order of the carrier frequency, and the influence of the QSM fields on the equation of electron motion cannot be neglected. In this case the analysis is no longer straightforward.

ACKNOWLEDGMENTS

We gratefully acknowledge X. T. He, C. Y. Zheng, L. H. Cao, Y. W. Tian, Z. J. Liu, B. Qiao, H. Y. Niu, S. Z. Wu, and J. Y. Wei for fruitful discussions. This work was supported by the National Hi-Tech Inertial Confinement Fusion (ICF) Committee of China, the NSF of China (NSFC) Grants No. 10135010, No. 10335020, No. 10375011, No. 10474081, No. 10575013, and No. 10576035, the Natural Science Foundation of Shanghai Project No. 05ZR14159, the Special Funds for Major State Basic Research Projects of China, and the Science Foundation of CAEP.

[1] J. A. Stamper, J. M. Dawson, K. Papadopoulos, R. N. Sudan, S. O. Dean, and E. A. Mclean, Phys. Rev. Lett. **26**, 1012 (1971).
[2] S. C. Wilks, W. L. Kruer, M. Tabak, and A. B. Langdon, Phys. Rev. Lett. **69**, 1383 (1992).
[3] R. N. Sudan, Phys. Rev. Lett. **70**, 3075 (1993).
[4] A. Pukhov and J. Meyer-ter-Vehn, Phys. Rev. Lett. **76**, 3975 (1996).
[5] M. Tatarakis, I. Watts, F. N. Beg, E. L. Clark, A. E. Dangor, A. Gopal, M. G. Haines, P. A. Norreys, U. Wagner, M.-S. Wei, M. Zepf, and K. Krushelnick, Nature (London) **415**, 280 (2002); M. Tatarakis *et al.*, Phys. Plasmas **9**, 2244 (2002).
[6] U. Wagner *et al.*, Phys. Rev. E **70**, 026401 (2004).
[7] A. Kim, M. Tushentsov, D. Anderson, and M. Lisak, Phys. Rev. Lett. **89**, 095003 (2002).
[8] V. I. Berezhiani, S. M. Mahajan, and N. L. Shatashvili, Phys.

Rev. E **55**, 995 (1997).
[9] M. G. Haines, Phys. Rev. Lett. **78**, 254 (1997); L. Gorbunov, P. Mora, and T. M. Antonsen, *ibid.* **76**, 2495 (1996).
[10] M. Borghesi, A. J. MacKinnon, A. R. Bell, R. Gaillard, and O. Willi, Phys. Rev. Lett. **81**, 112 (1998).
[11] Z. M. Sheng and J. Meyer-ter-Vehn, Phys. Rev. E **54**, 1833 (1996); M. D. Feit, A. M. Komashko, S. L. Musher, A. M. Rubenchik, and S. K. Turitsyn, *ibid.* **57**, 7122 (1998).
[12] A. R. Bell, J. R. Davies, and S. M. Guerin, Phys. Rev. E **58**, 2471 (1998).
[13] R. J. Mason and M. Tabak, Phys. Rev. Lett. **80**, 524 (1998).
[14] C. Y. Zheng, X. T. He, and S. P. Zhu, Phys. Plasmas **12**, 044505 (2005); S. P. Zhu, X. T. He, and C. Y. Zheng, *ibid.* **8**, 321 (2001).
[15] B. Qiao, S. P. Zhu, C. Y. Zheng, and X. T. He, Phys. Plasmas **12**, 053104 (2005).
[16] M. Tabak, J. Hammer, M. E. Glinsky, W. L. Kruer, S. C. Wilks, J. Woodworth, E. M. Campbell, and M. D. Perry, Phys. Plasmas **1**, 1626 (1994).
[17] R. Kodama *et al.*, Nature (London) **412**, 798 (2001).
[18] P. Goldreich and W. H. Julian, Astrophys. J. **157**, 869 (1969).
[19] W. Yu, M. Y. Yu, Z. M. Sheng, and J. Zhang, Phys. Rev. E **58**, 2456 (1998).
[20] H. B. Cai, W. Yu, S. P. Zhu, and C. Y. Zheng, Phys. Plasmas **13**, 113105 (2006).
[21] F. Cattani, A. Kim, D. Anderson, and M. Lisak, Phys. Rev. E **62**, 1234 (2000).
[22] A. Kim, M. Tushentsov, F. Cattani, D. Anderson, and M. Lisak, Phys. Rev. E **65**, 036416 (2002).
[23] P. Mora and T. M. Antonsen, Jr., Phys. Rev. E **53**, R2068 (1996).
[24] J. M. Kindel, K. Lee, and E. L. Lindman, Phys. Rev. Lett. **34**, 134 (1975).
[25] Z. M. Sheng, K. Mima, J. Zhang, and H. Sanuki, Phys. Rev. Lett. **94**, 095003 (2005); T. Speziale and P. J. Catto, Phys. Fluids **20**, 990 (1977).